ANTIMICROBIAL AGENTS AND CHEMOTHERAPY, Jan. 2008, p. 45–53 Vol. 52, No. 1
0066-4804/08/$08.00+0 doi:10.1128/AAC.00534-07

Mutated Response Regulator *graR* Is Responsible for Phenotypic Conversion of *Staphylococcus aureus* from Heterogeneous Vancomycin-Intermediate Resistance to Vancomycin-Intermediate Resistance▽

Hui-min Neoh,[1] Longzhu Cui,[1,2] Harumi Yuzawa,[1] Fumihiko Takeuchi,[2] Miki Matsuo,[1] and Keiichi Hiramatsu[1,2]*

Department of Bacteriology[1] and Department of Infection Control Science,[2] Faculty of Medicine, Juntendo University, 2-1-1 Bunkyo-Ku, Tokyo, Japan 113-8421

Received 23 April 2007/Returned for modification 7 May 2007/Accepted 9 October 2007

Multistep genetic alteration is required for methicillin-resistant *Staphylococcus aureus* (MRSA) to achieve the level of vancomycin resistance of vancomycin-intermediate *S. aureus* (VISA). In the progression of vancomycin resistance, strains with heterogeneous vancomycin resistance, designated hetero-VISA, are observed. In studying the whole-genome sequencing of the representative hetero-VISA strain Mu3 and comparing it with that of closely related MRSA strains Mu50 (VISA) and N315 (vancomycin-susceptible *S. aureus* [VSSA]), we identified a mutation in the response regulator of the *graSR* two-component regulatory system. Introduction of mutated *graR*, designated *graR, but not intact *graR*, designated *graRn*, could convert the hetero-VISA phenotype of Mu3 into a VISA phenotype which was comparable to that of Mu50. The same procedure did not appreciably increase the vancomycin resistance of VSSA strain N315, indicating that *graR** expression was effective only in the physiological milieu of hetero-VISA cell to achieve a VISA phenotype. Interestingly, the overexpression of *graR** increased the daptomycin MICs in both Mu3 and N315 and decreased the oxacillin MIC in N315.**

Vancomycin-intermediate *Staphylococcus aureus* (VISA), first described in 1997, has continuously been a worldwide problem in the treatment of methicillin-resistant *S. aureus* (MRSA) hospital infection (16). VISA has a unique mechanism of resistance; the resistant cell produces a thickened cell wall, whereby many vancomycin molecules are trapped within the cell wall. The trapped molecules clog the peptidoglycan meshwork and finally form a physical barrier towards further incoming vancomycin molecules (5, 6, 13). VISA does not directly emerge from vancomycin-susceptible MRSA. It emerges from hetero-VISA that expresses heterogeneous-type vancomycin resistance (14). Hetero-VISA spontaneously produces VISA cells within its cell population at a frequency of 10^{-6} or above (14). Using differential hybridization, we have identified the two-component system *vraSR*, which is constitutively activated in Mu50 (VISA) and Mu3 (hetero-VISA) but strongly depressed in vancomycin-susceptible *S. aureus* (VSSA) strain Mu50Ω (18). *vraSR* turned out to be an up-regulator of cell wall peptidoglycan synthesis (7). Its overexpression in VSSA strain N315 decreases VSSA's susceptibility to the level of hetero-VISA but not to the level of VISA (defined as a vancomycin MIC of ≥4 mg/liter). This study was conducted to search for the second genetic alteration that promotes hetero-VISA-to-VISA phenotypic conversion.

* Corresponding author. Mailing address: Department of Bacteriology, Faculty of Medicine, Juntendo University, 2-1-1 Hongo, Bunkyo-Ku, Tokyo, Japan 113-8421. Phone: (813) 3-5802-1040. Fax: (813) 3-5684-7830. E-mail: khiram06@med.juntendo.ac.jp.

▽ Published ahead of print on 22 October 2007.

MATERIALS AND METHODS

Bacterial strains. VISA strain Mu50 and hetero-VISA strain Mu3 have been described previously (14). N315, isolated in 1982 in Japan, is a prototype of Japanese hospital-associated MRSA strains with genotype IIA (type IIa SCC*mec* and multilocus sequence type 5), to which Mu3 and Mu50 belong (12). N315 is a pre-MRSA strain; that is, its expression of methicillin resistance is repressed due to the presence of an intact copy of the *mecI* gene encoding a *mecA* gene transcription repressor on the chromosome (21). A collection of 13 VISA strains from six countries was used for *graSR* sequencing. They were MI, NJ, and IL (isolated from the United States); AMC11094 (Korea); 99/3700 (United Kingdom); LIM2, 98141 (France); 28160 (South Africa); and BR1 to BR5 (Brazil). These strains have been described previously (8).

Recombinant DNA techniques and electroporation. Plasmid DNA was purified from *Escherichia coli* by use of an SV Minipreps DNA purification system (Promega Corporation, Madison, WI) according to the manufacturer's instructions. DNA isolation from *S. aureus* cells, restriction endonuclease digestion, ligation reactions, and DNA cloning were carried out as described previously (7). The electroporation of *S. aureus* was performed with a Bio-Rad gene pulser with a pulse controller as described previously (21). Recombinant plasmids p*graRn* and p*graR** were constructed by cloning into the pYT3 plasmid vector the PCR-amplified *graR* gene (SA0614) from N315 and Mu50 chromosomes, respectively, by use of the primers (5′-ttttt<u>ggatcc</u>GGATTAAAGATTTTCAAAGTC-3′) and (5′-ttttt<u>ggatcc</u>GAGATTTCAAAAAATAAGCTAC), in which the underlined parts represent added BamHI sites. The integrity of the cloned *graR* gene was ascertained by sequencing each recombinant plasmid. The resultant plasmids, p*graRn* and p*graR**, were then introduced into N315 and Mu3, resulting in strains N315(p*graRn*), N315(p*graR**), Mu3(p*graRn*), and Mu3(p*graR**). For the complementation of the *graSR*-knocked-out strain N315Δ*graSR* (see below), plasmid p*graSR** was used, which was constructed by cloning the *graSR* genes (SA0615 and SA0614) of Mu50 into pYT3. The *graSR** genes were PCR amplified with the Mu50 genomic DNA as a template by use of primer sets 5′-ttttt<u>ggatcc</u>TACATCTATACGATTATATC-3′ and 5′-ttttt<u>ggatcc</u>ACATATG ACTAACATCTATC-3′, in which the underlined parts represent added BamHI sites.

Construction of *graSR* knockout strains. The *graSR*-null knockout mutants of N315 and Mu3 were constructed by an allelic exchange method as described previously (7), with the exception that the 1.5-kb and 1-kb fragments of the left

TABLE 1. List of nucleotide differences between Mu3 and Mu50 chromosomes

No.[a]	Position on Mu50 chromosome	Nucleotide			Mu50 ORF	Gene	SNP or mismatched gene product	Amino acid change (Mu3 → Mu50)
		Mu50	Mu3	N315				
S-1	139748	G	C	C	SAV0124		Hypothetical protein, ParB-like nuclease	Ala → Gly
S-2	605306	T	C	C	SAV0542	*rpoB*	rpoB/RNA polymerase beta chain	His → Tyr
S-3	733083	G	A	A	SAV0659	*graR*	Two-component response regulator	Asn → Ser
S-4	1511305	A	C	C	SAV1429		Hypothetical protein	Asp → Tyr
S-5	2128392	A	G	G	SAV2005		Similar to leukocidin chain *lukM* precursor	Pro → Ser
S-6	2433955	A	G	G	SAV2309		Similar to formate dehydrogenase	Val → Ala
S-7	1372630	T	A	T	SAV1299		Hypothetical protein	Phe → Leu
S-8	1570869	C	T	C	SAV1455	*dinG*	Probable ATP-dependent DNA helicase	Asp → Gly
S-9	2264148	G	A	G	SAV2136	*pdp*	Pyrimidine nucleoside phosphorylase	Ile → Thr
S-10	206670	G	A	G	SAV0182	*argB*	*N*-Acetyl-L-glutamate 5-phosphotransferase	Glu → Glu
S-11	514468	A	G	G	SAV0471	*gltC*	Transcription activator of glutamate synthase operon	Ile → Ile
S-12	1693563	Del[b]	T	T	SAV1583	*hemN*	Oxygen-independent coproporphyrinogen oxidase	Stop → Stop
S-13	1798058	C	T	C	SAV1689		Hypothetical protein, formamidopyrimidine-DNA glycosylase	Ala → Ala
S-14	2557241	C	T	T	SAV2427	*bioD*	Dethiobiotin synthetase	Lys → Lys
S-15	1245994	G	A	G	Intergenic			
S-16	2070045	A	T	A	Intergenic			
M-1[c]	469796∼	Del	Intact	Intact		*set9*	Exotoxin 9	Del
M-2[d]	509791∼	Del	Intact	Intact	SAV0465	*sle1*	*N*-Acetylmuramyl-L-alanine amidase Sle1	Del
M-3[e]	2130907∼	Del	Intact	Intact	SAV2006		Hypothetical protein	Del

[a] "S-" stands for SNP, and "M-" for mismatch; for each difference, N315 chromosome information is given. There were a total of 16 SNPs between Mu50 and Mu3. chromosomes. Nine of them were missense mutations (S1 to S9), while the remaining 7 were silent mutations. S1 to S6 were Mu50 specific and S7 to S9 were Mu3 specific.
[b] Del, deletion.
[c] 1,242-bp nucleotide deletion in the Mu50 chromosome, resulting in the deletion of *set9*.
[d] 201-bp nucleotide deletion in Mu50, resulting in *sle1* gene truncation.
[e] 157-bp nucleotide deletion in Mu50, truncating the ORF SAV2006.

and right respective junctions of *graSR* were PCR amplified and cloned into the upstream and downstream regions of the *cat* gene of chloramphenicol resistance cassette vector pUC118cat (7). Since Mu3 is tetracycline resistant, the *graSR* knockout mutant of this strain was generated by the following protocol, also described by Bae and Schneewind (1). Briefly, the sequences flanking *graSR* were PCR amplified with primers attB1-KO614&5F (ggggacaagtttgtacaaaaaagcaggct GTAACTAAAAGGTGGAGTAA) and attB1-KO614&5R_SacII (TTTTTCCG CGGCCATATCACCCAATATCATT) for the upstream region and primers attB2-KO614&5F_SacII (TTTTTCCGCGGACATGCGTTTTGTTACTTAG) and attB2-KO614&5R (ggggaccactttgtacaagaaagctgggtGATAGATGGCATAA TGTGAT) for the downstream region. The PCR fragments were then ligated in vitro and recombined with pKOR1 (1). The pKOR1 recombinant was then introduced into *S. aureus* Mu3 by electroporation. Selection of the knockout strains was performed as described previously (1). The successful deletion of *graSR* genes was verified by sequence determination.

Whole-genome sequencing of Mu3 and its comparison with the Mu50 chromosome. Mu3 genome sequencing was performed as described previously (20), with shotgun sequencing with 6.4-fold coverage by use of a random small-insert library (1.5 to 2.5 kb). We used the chromosome sequence of Mu50 as a scaffold to assemble and orient Mu3 contigs, followed by gap closure using long-range PCR primer walking. We then compared the sequences of Mu3 and Mu50 chromosomes for single-nucleotide polymorphisms (SNPs) and mismatches. Identified discrepancies were verified by resequencing of the corresponding loci of Mu3 and Mu50 genomic DNAs. Open reading frame (ORF) prediction and gene annotation were performed as described previously (20). The entire Mu3 genome sequence and annotation have been deposited in DDBJ under accession number AP009324.

Electron microscopic evaluation of cell wall thickness. Preparation and examination of *S. aureus* cells by transmission electron microscopy were performed as described previously (9). Morphometric evaluation of cell wall thickness was performed using photographic images at a final magnification of ×30,000. One hundred thirty cells of each strain with nearly equatorial cut surfaces were measured for the evaluation of cell wall thickness, and results were expressed as mean values ± standard deviations.

Antibiotic susceptibility tests. The MIC determination was performed by agar dilution methods according to CLSI criteria (4). To detect small changes in susceptibility, linear sets of antibiotic concentrations with 1-mg/liter increments were adopted for the MIC determinations for vancomycin, teicoplanin, and daptomycin, whereas the orthodox twofold dilution system was used for oxacillin. Taking care not to miss a slow-growing resistant cell subpopulation of heterogeneous resistance expression, MIC was evaluated not only at 24 h but also at 48 h of incubation time (15).

RNA preparation and microarray analysis. Bacteria were grown in 10 ml of brain heart infusion (BHI) broth to exponential phase (optical density at 600 nm [OD_{600}] = 0.6) before harvest. Pellets were then suspended with precooled $T_{10}E_{10}$ buffer (10 mM Tris-HCl [pH 8.0]), followed by the addition of lysostaphin solution (WAKO, Japan) at a 3.0-μg/ml final concentration. The suspensions were then incubated at 37°C for 3 min until complete cell lysis occurred. Immediately, 7 ml of acidic phenol (pH 5.2, equilibrated with 20 mM sodium acetate) was added, followed by the addition of 600 μl of 3 M sodium acetate. The samples were then frozen (−80°C) and thawed (65°C) three times. Phenol-chloroform extraction and ethanol precipitation was then carried out. After that, the resulting RNA pellet was subjected to digestion with RNase-free DNase I

TABLE 2. MICs of *graSR*-derivative strains of N315 and Mu3[a]

Strain	MIC (mg/liter) of indicated antimicrobial at indicated time							
	Vancomycin		Teicoplanin		Oxacillin		Daptomycin	
	24 h	48 h	24 h	48 h	24 h	48 h	24 h	48 h
N315	0.5	0.5	1	1	2	8	0.5	0.5
N315(pYT3)	0.5	0.5	0.5	0.5	4	4	0.5	0.5
N315(p*graR**)	1	1	0.5	0.5	0.25	0.25	1	1
N315(p*graRn*)	0.5	0.5	0.5	0.5	0.5	1	0.5	0.5
N315Δ*graSR*	0.5	0.5	0.5	0.5	4	16	0.5	0.5
N315Δ*graSR*(p*graR**)	1	1	0.5	0.5	2	4	1	1
N315Δ*graSR*(p*graSR**)	1	1	0.5	0.5	0.5	0.5	1	1
Mu3	2	2	7	8	1,025	>1,025	1	1
Mu3(pYT3)	1	2	6	6	1,025	>1,025	1	2
Mu3(p*graR**)	4	4	6	7	1,025	1,025	3	3
Mu3(p*graRn*)	2	2	5	6	1,025	1,025	3	3
Mu3Δ*graSR*	1	1	3	4	1,025	1,025	0.5	0.5
Mu3Δ*graSR*(p*graR**)	3	4	6	6	1,025	1,025	3	3
Mu50	4	8	7	7	512	512	3	3

[a] The drug concentrations for oxacillin were twofold dilutions from 0.25 mg/liter to 1,025 mg/liter. For the other three antibiotics, tested concentrations were 0.5 mg/liter, 1 through 10 mg/liter with a 1-mg/liter increment, and a twofold dilution from 16 to 1,024 mg/liter.

(Roche, Mannheim, Germany) at 37°C for 30 min. The RNA samples were then purified again with phenol-chloroform extraction and ethanol precipitation. Pellets were then resuspended in 25 μl of diethyl pyrocarbonate-treated water. The construction and analysis of the DNA microarray have been previously described (7). To confirm reproducibility, RNA extraction and hybridization were performed in duplicate for each experiment. In addition, extractions of up-regulated and down-regulated genes in the Mu50/Mu3 combination were done using three independent experimental data to ensure a high level of credibility for the results. The values for transcription rates given in the Mu50/Mu3 array study are the averages of the three experiments.

Growth curve and autolysis assay. Growth curve and autolysis experiments were carried out in succession. An overnight culture of a tested strain was diluted 1/1,000 in 10 ml fresh BHI broth and grown at 37°C with 25-rpm shaking in a photorecording incubator (TN-2612; Advantec, Tokyo, Japan). The OD was monitored automatically every 2 min, and cells were grown to an OD_{600} of 1.2. Following this, the cells were cooled on ice for 10 min and then pelleted by centrifugation at 7,500 rpm for 5 min. Cells were then washed twice and resuspended with chilled 0.1 M phosphate-buffered saline buffer (pH 7.0). The cell suspension was then incubated at 30°C with continuous shaking at 25 rpm. The decrease in optical density was monitored every 2 min for 24 h with the same photorecording incubator as described above. For growth curve and doubling time determination, values for OD versus time in the exponential growth phases of each strain were plotted. Doubling times were then calculated as follows: doubling time = $[(t_2 - t_1) \times \log 2]/[\log OD_{600}$ at $t_2 - \log OD_{600}$ at $t_1]$.

RESULTS

Whole-genome sequence determination of Mu3 and its comparison with the Mu50 genome. We determined the whole-genome sequence of hetero-VISA strain Mu3 and compared it with those of Mu50 and N315. (The whole-genome sequence of Mu3 is available under accession no. AP009324 [20]). Table 1 summarizes the differences in the nucleotide sequences of Mu3, N315, and Mu50 chromosomes. Among 16 SNPs and three mismatches, we found a Mu50-specific missense mutation in *graR*, a two-component response regulator gene (Table 1). The gene was also present in the list of 17 genes whose increased transcription raises vancomycin resistance (7).

The *graR* mutation replaces the 197th Asn of GraR with Ser. Besides Mu50, comparative sequencing of *graSR* from 13 clinical VISA strains obtained from six countries identified two other missense mutations in 10 of the 13 strains: Ser_{79} to Phe (strain NJ) and Asp_{148} to Gln (strains 99/3700-W, LIM2, 98141, 28160, and BR1 to BR5). The other three strains, MI, IL, and AMC11094, shared the same *graR* with N315 and Mu3. In contrast, no mutation was found in the *graS* genes of the 13 strains. This frequent mutation in *graR* in VISA clinical strains prompted us to test the effect of mutation on vancomycin resistance.

Expression of the mutated *graR* of Mu50 affects MICs of glycopeptides, oxacillin, and daptomycin. To test the role of the mutation, we PCR amplified and cloned the mutated *graR* gene, designated *graR**, and intact *graR*, designated *graRn* (where "*n*" stands for N315), into shuttle vector pYT3, obtaining p*graR** and p*graRn.* These plasmids were then introduced into Mu3 and N315 by electroporation, and MICs were evaluated (Table 2). MICs were determined by an agar dilution method according to the CLSI guidelines (4), with an additional condition, i.e., MIC reading after 48 h of incubation (Table 2). The introduction of *graR** into Mu3 significantly increased the vancomycin MIC from 2 to 5 mg/liter (in BHI agar), which was comparable to that of VISA strain Mu50 (Table 2). The introduction of *graR** also increased the daptomycin MIC from 2 to 5 mg/liter, which was also comparable to that (6 mg/liter) of Mu50 (Table 2). In contrast, the introduction of the intact *graR* (*graRn*) into Mu3 did not raise vancomycin or daptomycin MICs appreciably. No significant increase was observed in vancomycin and teicoplanin MICs when *graR** was introduced into N315 (Table 2). However, there was a slight decrease in the oxacillin MIC and a slight increase in the daptomycin MIC. This curious phenomenon was not apparent with the introduction of *graRn* (Table 2).

Since N315 and Mu3 have intact *graSR* genes on the chromosome, deletion mutant strains N315Δ*graSR* and Mu3Δ*graSR* were constructed for the confirmation of the role of the two-component system in antibiotic resistance. The *graSR* deletion of Mu3 caused small decreases in the vancomycin and daptomycin MICs and rather significant decreases in the teicoplanin MICs (Mu3Δ*graSR* [Table 2]). However, no evident change was observed in the oxacillin MIC. On the other hand, the *graSR* knockout of N315 (N315Δ*graSR*) caused a small in-

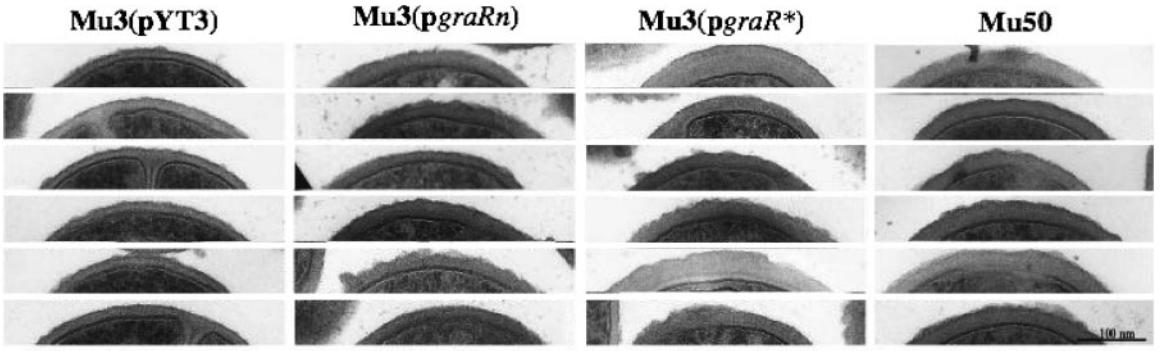

FIG. 1. Cell wall thickness of Mu3, Mu50, and *graR*-related Mu3 derivative strains Six representative transmission electron microscopy photos showing various cell wall thicknesses of each strain are presented. Mu3(p*graR**) showed a very thick cell wall (37.88 ± 11.31 nm), which was comparable to that of Mu50 (35.02 ± 4.01 nm) and was much thicker than that of Mu3(pYT3) (26.11 ± 3.66 nm). Mu3(p*graRn*) also showed increased cell wall thickness (32.50 ± 5.09 nm), but it was less significant than that of Mu3(p*graR**).

crease in the oxacillin MIC, while it did not affect the glycopeptide or daptomycin MICs appreciably (Table 2). Introduction of the plasmid p*graR** into Mu3Δ*graSR* raised its glycopeptide and daptomycin MICs to a level comparable to that seen for Mu3(p*graR**) (Table 2). On the other hand, the oxacillin and daptomycin MICs of N315Δ*graSR* were significantly affected downwards and upwards, respectively, with the introduction of p*graR**. A similar phenotypic change was observed for N315Δ*graSR*(p*graSR**), in which *graR** was introduced together with *graS* (Table 2). These data clearly indicated that the effect of introduced *graR** was not dependent on the presence of GraS in the cell.

Expression of *graR increases cell wall thickness and decreases growth rate and autolytic activity.** Transmission electron microscopy revealed that Mu3(p*graR**) showed remarkable cell wall thickening which was comparable to that of Mu50 (Fig. 1). In contrast, only a small degree of cell wall thickening was observed with Mu3(p*graRn*).

Mu3(p*graR**) also resembled Mu50 in terms of reduced autolytic activity (Fig. 2) and prolonged doubling time in drug-free medium (Fig. 3). Mu3(p*graRn*) also showed a slight reduction in autolytic activity and a prolonged doubling time. These changes, however, were not as significant as those seen for Mu3(p*graR**) (Fig. 2 and 3). Interestingly, the *graSR* knockout of Mu3 led to an enhanced autolytic activity and an accelerated growth rate (Fig. 2 and 3).

Expression of *graR in Mu3 increases the transcription of the genes that are specifically up-regulated in Mu50.** Figure 4 shows the results of three representative microarray analyses on *graR*-relevant derivative strains, including the one using strains Mu3(p*graR**) and Mu3(p*graRn*). Figure 4A shows the fluorescence intensities of all the array spots (left) and a scatter

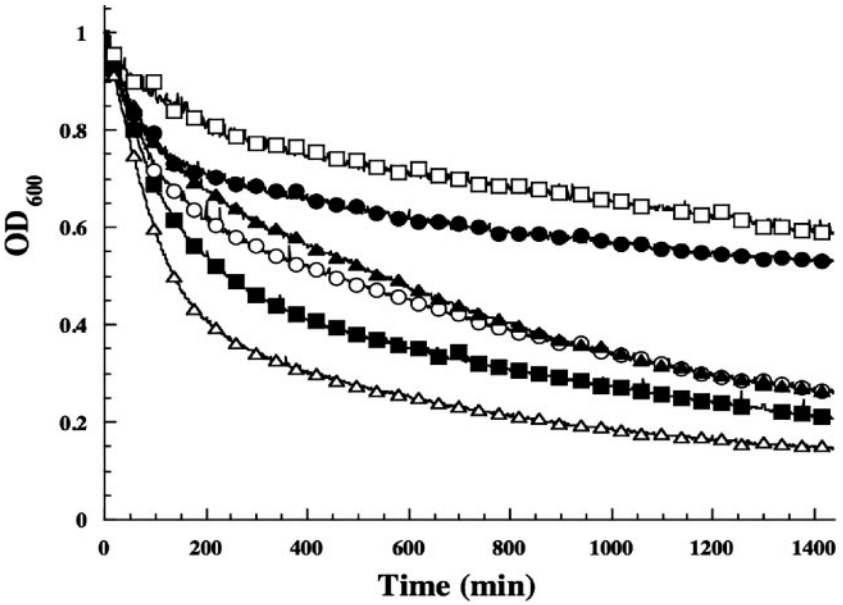

FIG. 2. Autolysis assay of Mu3, Mu50, and *graR*-related Mu3 derivative strains Symbols: open circles, Mu3; closed circles, Mu3(p*graR**); open triangles, Mu3Δ*graSR*; closed triangles, Mu3(p*graRn*); open squares, Mu50. Note that the introduction of p*graR** significantly decreased the autolysis activity of Mu3 to a level equal to that of Mu50. The autolysis of Mu3(p*graRn*) was also reduced but not as significantly as with Mu3(p*graR**). The deletion of *graSR* significantly enhanced the autolytic activity of Mu3.

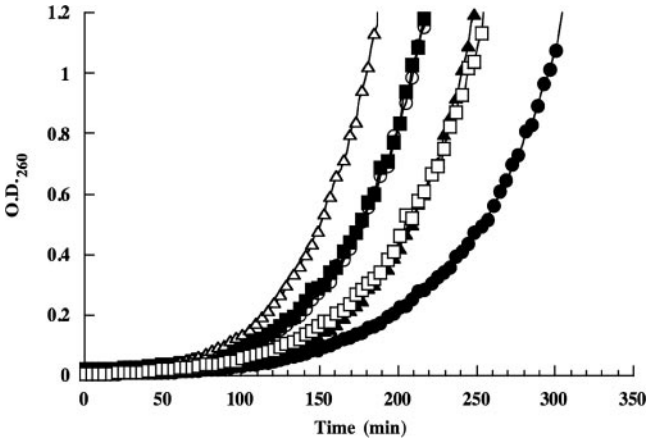

FIG. 3. Growth rates of Mu3, Mu50, and *graR*-related Mu3-derivative strains Symbols, strains, and doubling times (in minutes) are as follows: open circles, Mu3 (29.88); closed circles, Mu3(p*graR**) (41.52); open triangles, Mu3Δ*graSR* (26.66); closed triangles, Mu3 (p*graRn*) (30.12); open squares, Mu50 (34.27); closed squares, Mu3 (pYT3) (31.52). Note that the introduction of *graR** (and *graR*) decreased the growth rate of Mu3, while the deletion of *graSR* increased it.

diagram of normalized spot intensities in the study of Mu3 (p*graR**)/Mu3(p*graRn*) (right). The diagram shows seven spots whose signals were significantly high in strain Mu3(p*graR**) compared to the level for Mu3(p*graRn*). They correspond to the seven genes *vraFG*, *vraDE*, *isaB*, *mprF*(*fmtC*), and SAS091 (Fig. 4B, right). On the left of Fig. 4B is shown a magnified view of the signal intensities of these genes in three array experiments.

Table 3 summarizes the results of nine sets of array experiments performed in this study. The listed genes are the top 14 highly expressed genes in Mu50 compared to their expression in Mu3 (up-regulated genes), and the four most repressed genes in Mu50 relative to their expression in Mu3 (down-regulated genes). Criteria for the entry of up- and down-regulated genes were signal ratios of >1.7 and <0.5, respectively. The listed 14 up-regulated genes were those reproducibly found in the top 20 entries of three separate experiments.

As shown in Fig. 4 and in Table 3, 7 of the 14 up-regulated genes were found up-regulated in Mu3 when *graR**, but not the *graRn* gene, was overexpressed. *isaB* was enhanced in Fig. 4 but was not included in Table 3 because it was not enhanced in Mu50/Mu3. On the other hand, *glnR* and SAS091, found in the up-regulated gene list of the Mu50/Mu3 combination, were

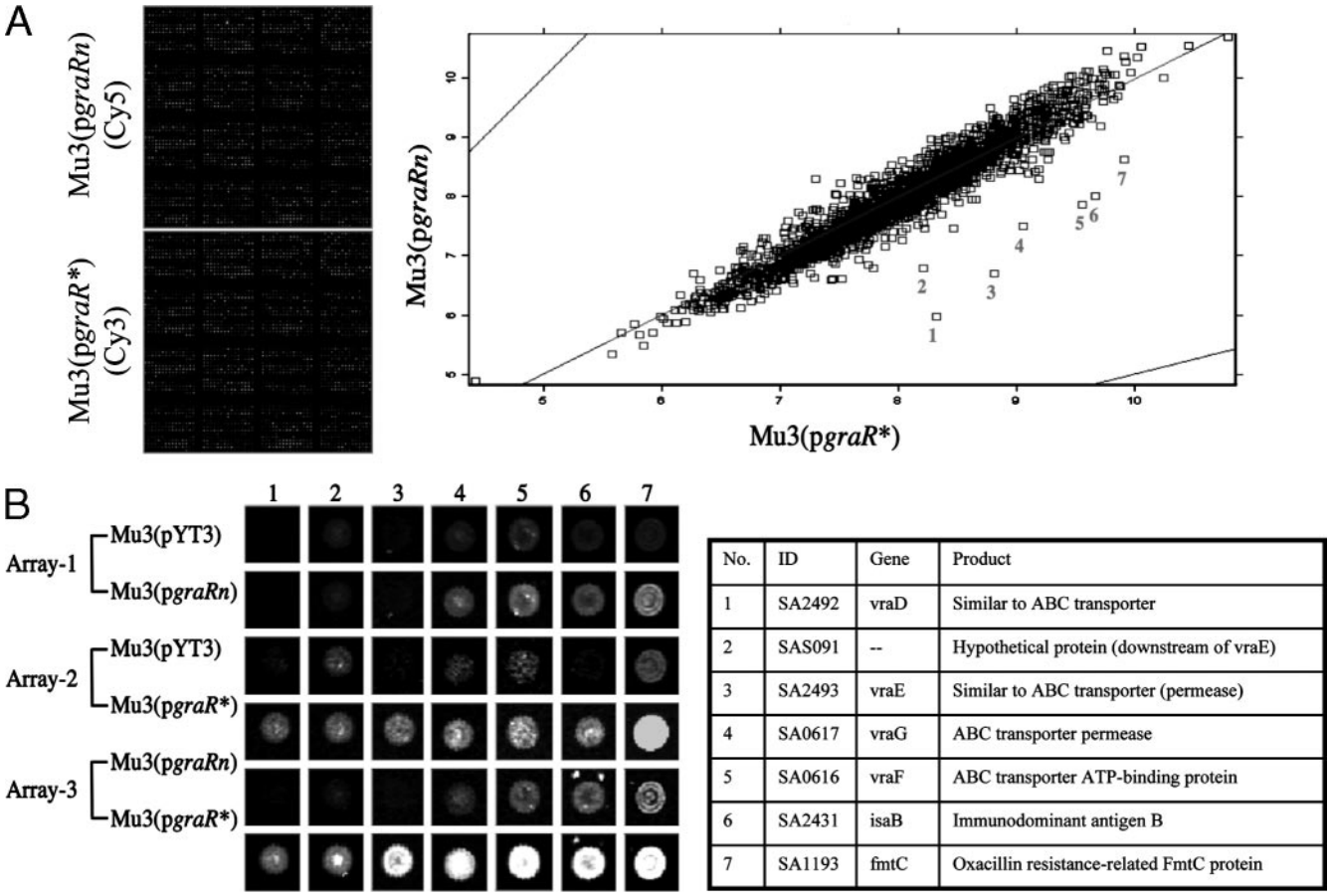

No.	ID	Gene	Product
1	SA2492	vraD	Similar to ABC transporter
2	SAS091	--	Hypothetical protein (downstream of vraE)
3	SA2493	vraE	Similar to ABC transporter (permease)
4	SA0617	vraG	ABC transporter permease
5	SA0616	vraF	ABC transporter ATP-binding protein
6	SA2431	isaB	Immunodominant antigen B
7	SA1193	fmtC	Oxacillin resistance-related FmtC protein

FIG. 4. Microarray image analysis for Mu3 *graR* transformants. Microarray image analysis was done using ImaGene 4.0 software (BioDiscovery, Inc. Los Angeles, CA) (A) (Left) Representative image of a microarray slide showing all florescence spots with different intensities; (right) scatter plot diagram of normalized spot intensities in the analysis of Mu3(p*graR**)/Mu3(p*graRn*). Seven spots were identified where the signal intensities were significantly higher in strain Mu3(p*graR**) than in Mu3(p*graRn*). (B) (Left) Magnified view of the above-described seven spots in three representative sets of microarray analysis; (right) the spots mentioned above correspond to the genes *vraFG*, *vraDE*, *isaB*, *fmtC*(*mprF*), and SAS091.

TABLE 3. Influence of *graR** expression on up- and down-regulated genes in VISA strain Mu50 relative to hetero-VISA strain Mu3

N315 ORFID	Gene name	Product[a]	Ratio of transcripts between strains of indicated combination[b]									
			Mu50/Mu3	Mu3(p*graR**)/Mu3(p*graRn*)	Mu3(p*graR**)/Mu3(pYT3)	Mu3(p*graRn*)/Mu3(pYT3)	Mu3Δ*graSR*/Mu3	Mu50/N315	N315(p*graR**)/N315(p*graRn*)	N315(p*graR**)/N315(pYT3)	N315Δ*graSR*/N315	Relative amt of transcripts[c]
Up-regulated												
SA0616	*vraF*	ABC transporter ATP-binding protein	**2.92**	**5.43**	**12.6**	1.59	0.89	**3.4**	**2.53**	1.35	1.16	Mu50 > Mu3 = N315
SA0617	*vraG*	ABC transporter permease	**2.26**	**4.48**	**9.98**	1.6	0.81	**5.71**	**2.55**	1.36	1.24	Mu50 > Mu3 > N315
SA2493	*vraE*	HP similar to ABC transporter permease	**2.16**	**13.9**	**6.04**	0.5	1.39	**66.9**	**3.91**	**7.05**	1.63	Mu50 > Mu3 ≫ N315
SAS091		HP	**2.06**	**3.5**	**1.84**	0.58	0.79	**13.7**	**2.84**	0.02	1.45	Mu50 > Mu3 ≫ N315
SA1713		HP similar to RNA methyltransferase	**1.99**	1.08	0.1	1.08	1.21	0.98	1.05	0.69	1.23	Mu50 > Mu3 = N315
SA1193	*mprF*	Lysylphospha-tidylglycerol synthetase	**1.88**	**2.79**	**7.48**	**2.38**	**0.49**	**1.8**	**1.79**	0.83	0.67	Mu50 > Mu3 = N315
SA1710		HP similar to DNA polymerase III, alpha chain PolC type	**1.87**	1.09	1.29	0.74	1.49	**3.89**	0.99	0.61	0.91	Mu50 > Mu3 > N315
SA1149	*glnR*	Glutamine synthetase repressor	**1.85**	**2.6**	**12.9**	1.16	0.82	**3.23**	1.33	1.05	1.4	Mu50 > Mu3 = N315
SA1030		CHP	**1.84**	1.41	1.21	1.06	0.82	1.03	**1.8**	0.48	0.79	Mu50 = N315 > Mu3
SA1082	*rimM*	Probable 16S rRNA-processing protein	**1.8**	0.74	1	0.91	1.19	0.72	0.84	0.72	1.44	Mu50 = N315 > Mu3
SA2492	*vraD*	HP similar to ABC transporter ATP-binding protein	**1.74**	**21**	**6.66**	0.77	**0.18**	**13.5**	**4.04**	**2.23**	0.57	Mu50 > Mu3 ≫ N315
SA1690		CHP	**1.74**	0.89	1.26	1.07	0.93	0.57	1.26	0.45	0.83	N315 > Mu50 > Mu3
SA0962		CHP	**1.73**	1.02	**1.92**	1.13	0.55	**3.28**	1.37	0.52	0.87	Mu50 > Mu3 > N315
SA1633		HP similar to beta-lactamase	**1.73**	1.34	0.99	0.63	1.23	**2.13**	0.65	0.29	1.22	Mu50 > Mu3 > N315
Reference genes												
SA2431	*isaB*	Immunodominant antigen B	1.21	**5.25**	**1.9**	**1.76**	0.78	**0.79**	1.69	1.1	0.56	Mu50 = Mu3 = N315
SA0615	*graS*	HP similar to two-component sensor histidine kinase	1.16	**1.98**	**1.63**	**1.68**	0.002	**0.66**	1.36	1.14	0.002	Mu50 = Mu3 = N315
SA0614	*graR*	HP similar to two-component response regulator	1.1	1.44	**16.1**	**29.1**	0.093	0.73	1.17	10.3	0.001	Mu50 = Mu3 = N315
SA1701	*vraS*	Two-component sensor histidine kinase	1.1	1.27	0.84	1.05	0.89	**1.97**	1.53	0.74	0.71	Mu50 = Mu3 > N315

SA1700	*vraR*	Two-component response regulator	1.05	1.12	1.5	0.99	0.81	**2.69**	1.19	0.55	0.64	Mu50 = Mu3 > N315
Down-regulated												
SA0055		CHP	0.37	1.27	0.15	0.94	0.45	EX[d]	0.87	EX	EX	
SA0058	*ccrA*	Cassette chromosome recombinase A	0.44	1.04	1.56	0.94	1.07	EX	1.02	0.04	EX	
SA0108	*sarH1* (*sarS*)	Staphylococcal accessory regulator A homologue	0.45	0.74	0.6	0.83	1.01	0.26	0.88	0.41	0.54	N315 > Mu3 > Mu50
SA0107	*spa*	Immunoglobulin G binding protein A precursor	0.47	0.75	0.45	0.77	1.03	0.29	0.65	0.57	0.59	N315 > Mu3 > Mu50

[a] HP, hypothetical protein; CHP, conserved hypothetical protein.
[b] Boldface indicates values either significant (<0.5 or >1.7) or referred to in the text.
[c] >, greater than 1.7-fold; ≫, greater than 2.89 (1.7 × 1.7)-fold; =, comparable; based on the experiments with Mu50/Mu3 and Mu50/N315.
[d] EX, excluded. Both the Cy3 and Cy5 signals were less than 0.1.

also found to be up-regulated in the Mu3(p*graR**)/Mu3(p*graRn*) combination (Table 3).

Comparison of the two array data for Mu3(p*graRn*)/Mu3 (pYT3) and Mu3(p*graR**)/Mu3(pYT3) clearly showed that the intact *graR* gene was unable to increase the transcription of these genes [except for *fmtC*(*mprF*), which gave a value of 2.38] (Table 3). A similar repertoire of genes was increased in transcription in the N315(p*graR**)/N315(p*graRn*) combination. However, the rates of increase of transcription were small with N315(p*graR**)/N315(pYT3) compared to what was seen for Mu3(p*graR**)/Mu3(pYT3), except that *vraDE* genes encoding a putative ABC transporter were significantly increased in both combinations. Therefore, the regulatory effect of *graR** was considered much stronger in Mu3 than in N315. Deletion of *graSR* of N315 and Mu3 decreased the transcription of only two of the seven up-regulated genes by *graR**. They were *fmtC*(*mprF*) and *vraD* (0.49- and 0.18-fold in Mu3 and 0.67- and 0.57-fold in N315, respectively), but the others (*vraFG*, *vraE*, SAS091, and *glnR*) were not affected much (0.79- to 1.40-fold) (Table 3). The data indicated that these genes were also regulated by some regulatory genes other than *graSR*.

DISCUSSION

The genetic mechanism of vancomycin resistance in VISA is not well understood. Several genes have been proposed as being involved in certain clinical VISA strains (2, 3, 17, 19, 22, 23). Since our first isolation of VISA strain Mu50 and hetero-VISA strain Mu3 from Juntendo University Hospital, we have been trying to understand the genetic process of vancomycin resistance acquisition in the Mu3-Mu50 lineage of strains. Mu3 and Mu50 have in common the characteristic of accelerated cell wall synthesis (11). Activation of the two-component system *vraSR*, which up-regulates the enzymes of the peptidoglycan synthesis pathway such as PBP2 and the *sgtB* and *murZ* products, etc., explains these features common to Mu3 and Mu50 (18). In fact, Mu3 and Mu50 share a common missense mutation in the *vraS* gene in the region corresponding to the N-terminal region (Asn5 → Ile), and its transcription is constitutively increased in both strains (18, 19) (K. Hiramatsu, unpublished observation). In this study, we identified a mutation in another two-component system, *graSR*. The mutation was located in the response regulator *graR*, and its expression in Mu3 caused remarkable cell wall thickening and an increase in the vancomycin MIC to the level seen for VISA strain Mu50. The overexpression of *graR** in N315 did not cause that significant effect on the level of vancomycin resistance or cell wall thickening (data not shown). This host difference in the expression of vancomycin resistance may well be explained by the fact that the enzymes of cell wall synthesis, such as PBP2 and the *sgtB* and *murZ* products, etc., are more abundant in Mu3 than in N315 due to the activated *vraSR* system in Mu3. Therefore, the mutated *graR* seems to confer the VISA phenotype only to cells that are producing cell wall peptidoglycan at an enhanced rate.

With regard to the physiological function of *graR**, our microarray experiments showed increased transcription of two sets of ABC transporter genes: *vraDE* and *vraFG*. It is therefore a tempting hypothesis to suggest that *graR** activates the membrane traffic of substrates for the cell wall synthesis en-

zymes to help them produce thickened cell wall peptidoglycan. Alternatively, *graR** might negatively regulate autolytic activity, thus allowing the cell wall peptidoglycan accumulate on the cell surface. This is also a plausible hypothesis, since deletion of *graSR* drastically increased autolytic activity in Mu3 (Fig. 2 and 3). It was also noted that *fmtC*(*mprF*) was among the seven genes whose transcription was significantly increased in Mu3(p*graR**) (Fig. 4 and Table 3).

Enhanced expression of the gene product lysylphosphatydylglycerol synthetase might contribute to vancomycin resistance by increasing the cell membrane positive charge and repulsing the positively charged vancomycin molecules (24, 25). The decreased growth rate of Mu3(p*graR**) compared to Mu3 may be a consequence of the reduced autolytic activity mediated by *graR** expression. More-detailed experiments would be needed to identify the regulatory role of the mutated as well as the intact *graSR* two-component system in the hetero-VISA-to-VISA conversion.

The *graR* mutation replaces Asn_{197} of GraR with Ser. In view of the signal transmission mechanism of the bacterial two-component system, the conformational change of the GraR protein by the mutation might have activated its response regulator function without signal input from the signal transducer GraS. This is predicted from the complementation experiment with *graSR* knockout strains (Table 2). Since the function of *graR** in altering antibiotic MICs was observed in the absence of the signal transducer GraS, it is probable that at least a part of the GraR* proteins was already active without activation through phosphorylated GraS proteins. The activation may occur either via an increased chance of autophosphorylation of GraR* or by a structural mimicry of the conformational change of GraR brought about by GraS-mediated phosphorylation. Another possibility is that GraR* may be activated by some of the other 15 two-component signal transducers known to be present in the *S. aureus* chromosome (20). Detailed studies on the *graSR* activation mechanism are under way to solve the question.

Reduced daptomycin susceptibility is highly correlated with the vancomycin resistance of VISA clinical strains (10). The expression of *graR** in Mu3 increased not only vancomycin resistance but also daptomycin resistance. This provided solid evidence that at least a part of the mechanism of vancomycin resistance is shared by the mechanism of daptomycin resistance.

It was also noticed that *graR** affected oxacillin resistance negatively when introduced in N315 (Table 2). This phenomenon reminds us of the "see-saw phenomenon," which occurs in certain stages of vancomycin resistance promotion (26). It is possible that *graSR* activation is the underlying genetic event for the phenomenon. N315 is called pre-MRSA, since its *mecA* gene expression is strongly repressed by the presence of the intact *mecA* repressor gene *mecI* (21). The *mecI* gene was among the down-regulated genes in our microarray data with the N315Δ*graSR*/N315 combination (the ratio of transcription was 0.26). The phenotypic expression of the raised oxacillin resistance in N315Δ*graSR* was not of an Eagle type (defined by resistance to high but not to low concentrations of oxacillin, a phenotypic expression caused by the presence of an intact *mecI* gene) (21). Therefore, the raised resistance in N315Δ*graSR* was consistent with the lifting of *mecI* gene-mediated repression of the *mecA* gene. However, the contribution of *graSR* on *mecI* gene regulation seemed complex. For example, the overexpression of *graR** in N315 did not increase the *mecI* gene transcript level (data not shown). Therefore, the effect of *graSR* on *mecI* gene transcription does not seem to occur in a simple colinear fashion. Further study is required to elucidate the relationship between *mecA* gene expression and *graR** expression.

Although many questions arose and remain to be answered, we provided the first glimpse of the genetic alterations underlying the hetero-VISA-to-VISA promotion of vancomycin resistance naturally occurring in hospitals. The mechanism may not apply to all VISA strains. However, the physiological outcome of the genetic alteration underlying the VISA phenotype is expected to be similar, i.e., increased peptidoglycan synthesis and accumulation of cell wall materials on the cell surface. To achieve this conversion at high frequency within the cell population exposed to vancomycin, *S. aureus* cells seem to utilize "regulator gene mutations" (17). Regulator gene function can be affected by mutation in many different ways. Some mutations may cause complete inactivation of the regulator function or may partially inactivate it to various degrees depending on the position and nature of mutation (substitution to different amino acids) in the coding region. In this study, we found a curious example of regulator mutation that seems to activate or alter its regulatory function. Compared to VRSA, where a simple intake of the genetic system (*vanA*, *vanH*, *vanY*, and *vanX*) completes the drastic alteration of cell wall peptidoglycan composition, the acquisition of vancomycin resistance by VISA is based on spontaneous mutation. Dozens of mutations would be needed to achieve a VISA phenotype by activating transcription of each of the many enzymes and transporters involved in the cell wall synthesis pathway. This may be the reason why regulator gene mutations have a significant biological meaning. Microarray experiments revealed that a single mutation in *vraS* or *graR* alters the expression of more than 100 genes, thus causing an extreme perturbation of cell homeostasis towards the generation of cells with novel equilibrium that fits the new adverse environment. The Mu3-Mu50 lineage of strains used mutations in two sets of two-component regulatory systems, *vraSR* and *graSR*, to generate a VISA genotype to survive vancomycin chemotherapy.

ACKNOWLEDGMENTS

We thank Taeok Bae for providing us the plasmid pKOR1.

This work was supported by a grant-in-aid for 21st century COE research and a grant-in-aid for scientific research (18590438) from The Ministry of Education, Science, Sports, Culture and Technology of Japan.

REFERENCES

1. **Bae, T., and O. Schneewind.** 2006. Allelic replacement in *Staphylococcus aureus* with inducible counter-selection. Plasmid **55:**58–63.
2. **Bischoff, M., M. Roos, J. Putnik, A. Wada, P. Glanzmann, P. Giachino, P. Vaudaux, and B. Berger-Bachi.** 2001. Involvement of multiple genetic loci in *Staphylococcus aureus* teicoplanin resistance. FEMS Microbiol. Lett. **194:**77–82.
3. **Boyle-Vavra, S., B. L. de Jonge, C. C. Ebert, and R. S. Daum.** 1997. Cloning of the *Staphylococcus aureus ddh* gene encoding NAD^+-dependent D-lactate dehydrogenase and insertional inactivation in a glycopeptide-resistant isolate. J. Bacteriol. **179:**6756–6763.
4. **Clinical and Laboratory Standards Institute.** 2006. Performance standards for antimicrobial susceptibility testing; sixteenth informational supplement, vol. 26, no. 3. M100–S16. Clinical and Laboratory Standards Institute, Wayne, PA.

5. **Cui, L., and K. Hiramatsu.** 2003. Vancomycin-resistant *Staphylococcus aureus*, p. 187–212. *In* A. C. Fluit and F. J. Schmitz (ed.), MRSA: current perspectives. Caister Academic Press, Norfolk, England.
6. **Cui, L., A. Iwamoto, J. Q. Lian, H. M. Neoh, T. Maruyama, Y. Horikawa, and K. Hiramatsu.** 2006. Novel mechanism of antibiotic resistance originating in vancomycin-intermediate *Staphylococcus aureus*. Antimicrob. Agents Chemother. **50:**428–438.
7. **Cui, L., J. Lian, H. Neoh, R. Ethel, and K. Hiramatsu.** 2005. DNA microarray-based identification of genes associated with glycopeptide resistance in *Staphylococcus aureus*. Antimicrob. Agents Chemother. **49:**3404–3413.
8. **Cui, L., X. Ma, K. Sato, K. Okuma, F. C. Tenover, E. M. Mamizuka, C. G. Gemmell, M. N. Kim, M. C. Ploy, N. El-Solh, V. Ferraz, and K. Hiramatsu.** 2003. Cell wall thickening is a common feature of vancomycin resistance in *Staphylococcus aureus*. J. Clin. Microbiol. **41:**5–14.
9. **Cui, L., H. Murakami, K. Kuwahara-Arai, H. Hanaki, and K. Hiramatsu.** 2000. Contribution of a thickened cell wall and its glutamine nonamidated component to the vancomycin resistance expressed by *Staphylococcus aureus Mu50*. Antimicrob. Agents Chemother. **44:**2276–2285.
10. **Cui, L., E. Tominaga, H. M. Neoh, and K. Hiramatsu.** 2006. Correlation between reduced daptomycin susceptibility and vancomycin resistance in vancomycin-intermediate *Staphylococcus aureus*. Antimicrob. Agents Chemother. **50:**1079–1082.
11. **Hanaki, H., K. Kuwahara-Arai, S. Boyle-Vavra, R. S. Daum, H. Labischinski, and K. Hiramatsu.** 1998. Activated cell-wall synthesis is associated with vancomycin resistance in methicillin-resistant *Staphylococcus aureus* clinical strains Mu3 and Mu50. J. Antimicrob. Chemother. **42:**199–209.
12. **Hiramatsu, K.** 1995. Molecular evolution of MRSA. Microbiol. Immunol. **39:**531–543.
13. **Hiramatsu, K.** 2001. Vancomycin-resistant *Staphylococcus aureus*: a new model of antibiotic resistance. Lancet Infect. Dis. **1:**147–155.
14. **Hiramatsu, K., N. Aritaka, H. Hanaki, S. Kawasaki, Y. Hosoda, S. Hori, Y. Fukuchi, and I. Kobayashi.** 1997. Dissemination in Japanese hospitals of strains of *Staphylococcus aureus* heterogeneously resistant to vancomycin. Lancet **350:**1670–1673.
15. **Hiramatsu, K., M. Kapi, Y. Tajima, L. Cui, S. Trakulsomboon, and T. Ito.** 2004. Advance in vancomycin-resistance research in *Staphylococcus aureus*, p. 289–298. *In* M. Alekshun, P. McDermott, and D. White (ed.), Frontiers in antibiotic resistance: a tribute to Stuart B. Levy. ASM Press, Washington DC.
16. **Hiramatsu, K., K. Okuma, X. X. Ma, M. Yamamoto, S. Hori, and M. Kapi.** 2002. New trends in *Staphylococcus aureus* infections: glycopeptide resistance in hospital and methicillin resistance in the community. Curr. Opin. Infect. Dis. **15:**407–413.
17. **Jansen, A., M. Turck, C. Szekat, M. Nagel, I. Clever, and G. Bierbaum.** 2007. Role of insertion elements and yycFG in the development of decreased susceptibility to vancomycin in *Staphylococcus aureus*. Int. J. Med. Microbiol. **297:**205–215.
18. **Kuroda, M., H. Kuroda, T. Oshima, F. Takeuchi, H. Mori, and K. Hiramatsu.** 2003. Two-component system VraSR positively modulates the regulation of cell-wall biosynthesis pathway in *Staphylococcus aureus*. Mol. Microbiol. **49:**807–821.
19. **Kuroda, M., K. Kuwahara-Arai, and K. Hiramatsu.** 2000. Identification of the up- and down-regulated genes in vancomycin-resistant *Staphylococcus aureus* strains Mu3 and Mu50 by cDNA differential hybridization method. Biochem. Biophys. Res. Commun. **269:**485–490.
20. **Kuroda, M., T. Ohta, I. Uchiyama, T. Baba, H. Yuzawa, I. Kobayashi, L. Cui, A. Oguchi, K. Aoki, Y. Nagai, J. Lian, T. Ito, M. Kanamori, H. Matsumaru, A. Maruyama, H. Murakami, A. Hosoyama, Y. Mizutani-Ui, N. K. Takahashi, T. Sawano, R. Inoue, C. Kaito, K. Sekimizu, H. Hirakawa, S. Kuhara, S. Goto, J. Yabuzaki, M. Kanehisa, A. Yamashita, K. Oshima, K. Furuya, C. Yoshino, T. Shiba, M. Hattori, N. Ogasawara, H. Hayashi, and K. Hiramatsu.** 2001. Whole genome sequencing of meticillin-resistant *Staphylococcus aureus*. Lancet **357:**1225–1240.
21. **Kuwahara-Arai, K., N. Kondo, S. Hori, E. Tateda-Suzuki, and K. Hiramatsu.** 1996. Suppression of methicillin resistance in a *mecA*-containing pre-methicillin-resistant *Staphylococcus aureus strain* is caused by the *mecI*-mediated repression of PBP2′ production. Antimicrob. Agents Chemother. **40:**2680–2685.
22. **Maki, H., N. McCallum, M. Bischoff, A. Wada, and B. Berger-Bachi.** 2004. *tcaA* inactivation increases glycopeptide resistance in *Staphylococcus aureus*. Antimicrob. Agents Chemother. **48:**1953–1959.
23. **Milewski, W. M., S. Boyle-Vavra, B. Moreira, C. C. Ebert, and R. S. Daum.** 1996. Overproduction of a 37-kilodalton cytoplasmic protein homologous to NAD^+-linked D-lactate dehydrogenase associated with vancomycin resistance in *Staphylococcus aureus*. Antimicrob. Agents Chemother. **40:**166–172.
24. **Nishi, H., H. Komatsuzawa, T. Fujiwara, N. McCallum, and M. Sugai** 2004. Reduced content of lysyl-phosphatidylglycerol in the cytoplasmic membrane affects susceptibility to moenomycin, as well as vancomycin, gentamicin, and antimicrobial peptides, in *Staphylococcus aureus*. Antimicrob. Agents Chemother. **48:**4800–4807.
25. **Ruzin, A., A. Severin, S. L. Moghazeh, J. Etienne, P. A. Bradford, S. J. Projan, and D. M. Shlaes.** 2003. Inactivation of *mprF* affects vancomycin susceptibility in *Staphylococcus aureus*. Biochim. Biophys. Acta **1621:**117–121.
26. **Sieradzki, K., and A. Tomasz.** 1997. Inhibition of cell wall turnover and autolysis by vancomycin in a highly vancomycin-resistant mutant of *Staphylococcus aureus*. J. Bacteriol. **179:**2557–2566.